Published in final edited form as:
Heart Rhythm. 2007 December ; 4(12): 1565–1567.

Noninvasive Electrocardiographic Imaging (ECGI) of Scar-Related Atypical Atrial Flutter

Yong Wang, MS[a,d], **Richard B. Schuessler, PhD**[a,b], **Ralph J. Damiano, MD**[a,b], **Pamela K. Woodard, MD**[a,c], and **Yoram Rudy, PhD**[a,c,d]

a*Cardiac Bioelectricity and Arrhythmia Center (CBAC), Washington University in St Louis, St Louis, Missouri*

b*Division of Cardiothoracic Surgery, Washington University School of Medicine, St. Louis, Missouri*

c*Mallinckrodt Institute of Radiology, Washington University School of Medicine, St. Louis, Missouri*

d*Department of Biomedical Engineering,, Washington University in St Louis, St Louis, Missouri*

INTRODUCTION

Atrial arrhythmias, including atrial fibrillation, atrial flutter and other types of atrial tachycardia are common in humans. For instance, atrial fibrillation affects 0.5-1% of the general population, and more than 6% of people over 80 years old.[1] Knowledge of electrophysiological properties of the underlying atrial substrate can improve diagnosis and treatment of these arrhythmias. However, until recently a noninvasive method for imaging cardiac electrophysiology and arrhythmias has not been available. Electrocardiographic Imaging (ECGI) was developed for this purpose.[2,3] ECGI reconstructs an epicardial electro-anatomical map noninvasively by combining a 250-electrode body surface ECG with CT scan of the heart-torso geometry. The ECGI images can be presented as epicardial potential maps, electrograms, isochrones or repolarization maps during activation and repolarization.[2,3] ECGI was systematically tested and validated experimentally in normal and abnormal canine hearts.[4-8] In these experimental settings, torso potentials (the ECGI input) and epicardial potentials (the ECGI output) were measured simultaneously and at high spatial and temporal resolution. The directly measured epicardial potentials provided the ideal "gold standard" for validation of the noninvasive ECGI reconstructions; We evaluated and validated the performance of ECGI under many different conditions, including ECGI of myocardial scars[5,6] and reentry circuits[4,6], the electrophysiological elements imaged in this report.

Recently, ECGI has also been successfully applied and validated in human subjects, including comparison to intra-operative multi-electrode mapping during surgery[9], determination of ECGI accuracy in locating focal sites of initial activation in humans by comparison to known locations of pacing electrodes in various RV and LV positions[2,10], comparison to catheter-based localization of focal VT[11] and determination of the origin of human atrial tachycardia

Address correspondence to: **Yoram Rudy, PhD.**, Cardiac Bioelectricity Center, 290 Whitaker Hall, Campus Box 1097, One Brookings Dr., Saint Louis, Missouri 63130-4899, Tel : (314)935-8160, Fax : (314)935-8168, Email : rudy@wustl.edu.

Dr. Rudy received stocks and stock options in Cardio Insight that develops ECGI for clinical use. But, none in conjunction with this study. He is an inventor on patents related to ECGI owned by Case Western Reserve and by Washington Universities. Dr. Wang is an inventor on a ptent related to EÇGI that is submitted and owned by Case Western Reserve University and Washington University

[12] In this case report, we describe the atrial substrate and arrhythmia mechanism of atypical atrial flutter in a patient who previously underwent catheter ablations for atrial fibrillation.

PATIENT HISTORY

The patient is a 48-year-old male with a two-year history of paroxysmal atrial fibrillation, unresponsive to multiple drug therapy. When not in atrial fibrillation, the patient had marked bradycardia, suggestive of sinus node dysfunction. He underwent catheter-based pulmonary vein (PV) isolation. After his first catheter ablation, the patient developed atypical atrial flutter. During this tachycardia, he had ventricular rates of 130 to 140 beats per minute. The patient's negative F-waves on Lead I were consistent with a left atrial (LA) origin of this tachycardia. Four months after the first ablation, he underwent a second procedure which revealed an inducible tricuspid isthmus-dependent atrial flutter and inducible LA reentry. The PVs were re-isolated and complete electrical isolation was documented. Additional ablations were made in the left side of the mitral isthmus, on the LA roof, and on the right side of the tricuspid IVC isthmus. Atrial flutter was not inducible following these ablations. Three months after the second ablation, the patient redeveloped persistent atypical atrial flutter. He was referred for a surgical COX-MAZE procedure after unsuccessful cardioversion.

METHODS

Body-surface ECG data were recorded for 5 minutes from 250 carbon electrodes mounted in strips. ECGI reconstructions were performed during beats with relatively long RR interval for which the atrial F wave was not masked by the QRS, and also for a 10 seconds ECG segment from which the QRST was removed. [13] Following the QRST removal, the ECG had a typical sawtooth morphology, and the ECGI-reconstructed atrial activation sequence was repetitious and consistent with only minor variations between cycles.

RESULTS

One day before the COX-MAZE procedure, ECGI was performed. Based on the magnitudes of the ECGI reconstructed epicardial electrograms, the atrial tissue was classified in terms of its electrophysiological properties. ECGI images showed low potential regions (electrogram magnitude <0.5mV peak to peak; Figure 1A) around each of the PVs and in the left atrial appendage (LAA) region. At surgery, scar tissue was observed around the PVs and on the LAA (Figure 1B), which corresponded well with the low voltage regions imaged by ECGI. Figure 1C shows two selected ECGI electrograms, one from the scar region (b) and one from a region remote to the scar (a).

ECGI-imaged activation sequence for one flutter cycle is shown in Figure 2. The reentry circuit driving the atypical flutter was mainly confined to the left atrium (LA). The circuit is depicted by the solid black and white arrows in the four panels of Figure 2. Earliest activation occurred at the LA inferior region below the left inferior PV (LIPV) (site 1). The activation front propagated posteriorly towards the right atrium (site 2) as indicated by the solid white arrows in Panel A and B. It could not propagate superiorly due to a line of block connecting the two inferior PVs (thick black line), associated with the posterior scar from the previous catheter ablations. This line of block extended to the anterior LA (Panel C). After about 50ms delay due to slow conduction at the border of the low potential region near the two right PVs (white arrow, Panel B), the activation wavefront turned around the line of block into the previously unexcited superior region (site 3). The reentrant wavefront continued to propagate towards the roof of the LA (site 4). From the LA roof, the wavefront propagated to anterior site 7, both directly and via the left atrial appendage (LAA) (site 6) (Panels C and D), and continued to the inferior mitral valve region (MV; site 8). It passed the MV isthmus, completing the reentry

circuit (Panels C and D). The next flutter cycle started again from site 1. A secondary wavefront emerged from the reentry circuit and propagated mainly in the right atrium (RA) (dashed black arrows in Panels B, C and D). It descended from the roof of the LA (site 4) to the inferior portion of RA free wall (site 5). There was a long line of functional block between site 2 and site 5 (thick black line in Panel B) due to refractoriness.

SUMMARY

We report the first application of ECGI in a patient with atypical atrial flutter that developed after catheter ablation for PV isolation. ECGI detected and mapped regions of low voltages that coincided with scar tissue around the pulmonary veins from the previous catheter ablation procedures, as verified during a COX-MAZE surgical procedure. The flutter reentry circuit was constrained by the scar and mainly confined to the LA. The mitral isthmus between the coronary sinus and the PVs participated in the reentry circuit. ECGI also imaged a region of low potentials on the let atrial appendage (LAA), which is uncommon. Typically, the LAA is a region of high voltage, as measured by endocardial mapping. During the COX-MAZE procedure it was observed that the LAA is extensively scarred (due to the underlying disease, not prior ablation), consistent with the ECGI reconstruction of low voltages in this region. The case reported in this manuscript was unique from the ECGI perspective, because prior to the COX-MAZE procedure the diagnosis was atrial fibrillation. ECGI constructed a monomorphic stable reentrant activation pattern that was repeated for many beats, indicating anatomical rather than functional reentry. Both ECGI reconstruction of low potentials and direct observation during surgery consistently identified an extensive scar around which the ECGI reconstructed isochrones formed the reentry circuit; the scar provided the anatomical substrate that stabilized the reentry. The repeatability of the reentry pattern over many beats demonstrates the consistency of ECGI methodology. It should be recognized that ECGI generates the entire activation map during a single beat and is therefore well suited to detect beat-to-beat changes during an arrhythmia. In contrast, catheter mapping (e.g. CARTO) is conducted point-by-point in a roving-prove fashion and requires data from many beats to construct an activation map. As such, it cannot provide data for comparison to ECGI in most cases. Following the COX-MAZE procedure, the patient returned to normal sinus rhythm.

Acknowledgements

This study was supported by NIH-NHLBI Merit Award R37-HL-33343 and Grant R01-HL-49054 (to Yoram Rudy). Yoram Rudy is the Fred Saigh distinguished professor at Washington University in St Louis. We also thank Li Li, Subham Ghosh and Lina EI-Esber for their help in the study.

References

1. Fuster V, Ryden LE, Asinger RW, Cannom DS, Crijns HJ, Frye RL, Halperin JL, Kay GN, Klein WW, Levy S, McNamara RL, Prystowsky EN, Wann LS, Wyse DG, Gibbons RJ, Antman EM, Alpert JS, Faxon DP, Gregoratos G, Hiratzka LF, Jacobs AK, Russell RO, Smith SC Jr, Alonso-Garcia A, Blomstrom-Lundqvist C, de Backer G, Flather M, Hradec J, Oto A, Parkhomenko A, Silber S, Torbicki A. ACC/AHA/ESC Guidelines for the Management of Patients With Atrial Fibrillation: Executive Summary A Report of the American College of Cardiology/American Heart Association Task Force on Practice Guidelines and the European Society of Cardiology Committee for Practice Guidelines and Policy Conferences (Committee to Develop Guidelines for the Management of Patients With Atrial Fibrillation) Developed in Collaboration With the North American Society of Pacing and Electrophysiology. Circulation 2001;104:2118–50. [PubMed: 11673357]
2. Ramanathan C, Ghanem RN, Jia P, Ryu K, Rudy Y. Noninvasive electrocardiographic imaging for cardiac electrophysiology and arrhythmia. Nat Med 2004;10:422–8. [PubMed: 15034569]
3. Ramanathan C, Jia P, Ghanem RN, Ryu K, Rudy Y. Activation and repolarization of the normal human heart under complete physiological conditions. Proc Natl Acad Sci USA (PNAS) 2006;103:6309–6314.

4. Burnes JE, Taccardi B, Rudy Y. A noninvasive imaging modality for cardiac arrhythmias. Circulation 2000;102:2152–8. [PubMed: 11044435]

5. Burnes JE, Taccardi B, MacLeod RS, Rudy Y. Noninvasive ECG imaging of electrophysiologically abnormal substrates in infarcted hearts: A model study. Circulation 2000;101:533–40. [PubMed: 10662751]

6. Burnes JE, Taccardi B, E PR, Rudy Y. Noninvasive electrocardiogram imaging of substrate and intramural ventricular tachycardia in infarcted hearts. Journal of the American College of Cardiology 2001;38:2071–8. [PubMed: 11738317]

7. Burnes JE, Ghanem RN, Waldo AL, Rudy Y. Imaging dispersion of myocardial repolarization, I: comparison of body-surface and epicardial measures. Circulation 2001;104:1299–305. [PubMed: 11551883]

8. Ghanem RN, Burnes JE, Waldo AL, Rudy Y. Imaging dispersion of myocardial repolarization, II: noninvasive reconstruction of epicardial measures. Circulation 2001;104:1306–12. [PubMed: 11551884]

9. Ghanem RN, Jia P, Ramanathan C, Ryu K, Markowitz A, Rudy Y. Noninvasive electrocardiographic imaging (ECGI): comparison to intraoperative mapping in patients. Heart Rhythm 2005;2:339–54. [PubMed: 15851333]

10. Jia P, Ramanathan C, Ghanem RN, Ryu K, Varma N, Rudy Y. Electrocardiographic imaging of cardiac resynchronization therapy in heart failure: Observation of variable electrophysiologic responses. Heart Rhythm 2006;3:296–310. [PubMed: 16500302]

11. Intini A, Goldstein RN, Jia P, Ramanathan C, Ryu K, Giannattasio B, Gilkeson R, Stambler BS, Brugada P, Stevenson WG, Rudy Y, Waldo AL. Electrocardiographic imaging (ECGI), a novel diagnostic modality used for mapping of focal left ventricular tachycardia in a young athlete. Heart Rhythm 2005;2:1250–2. [PubMed: 16253916]

12. Wang Y, Cuculich PS, Woodard PK, Lindsay BD, Rudy Y. Focal Atrial Tachycardia after Pulmonary Vein Isolation: Noninvasive Mapping with Electrocardiographic Imaging (ECGI). Heart Rhythm 2007;4:1081–1084. [PubMed: 17675084]

13. Xi Q, Sahakian AV, Swiryn S. The effect of QRS cancellation on atrial fibrillatory wave signal characteristics in the surface electrocardiogram. J Electrocardiol 2003;36:243–9. [PubMed: 12942487]

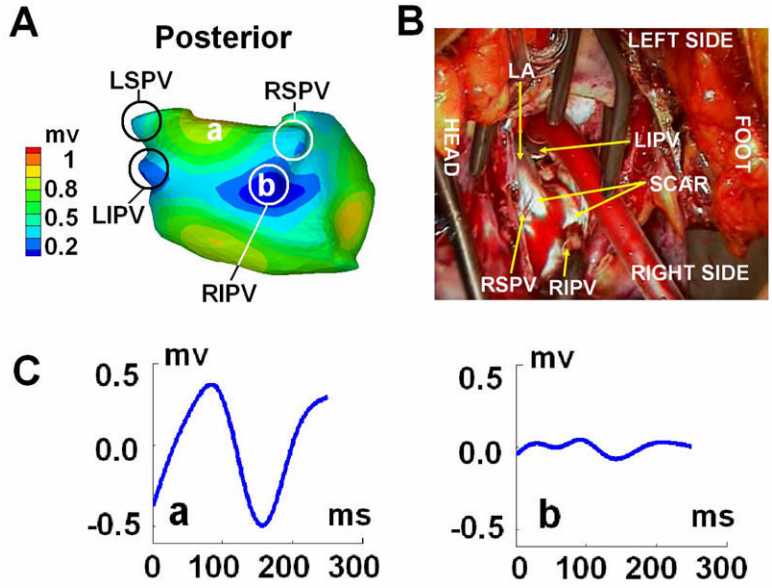

Figure 1.

Panel A: ECGI epicardial electrogram magnitude map (posterior view). Small magnitude regions (<0.5mV; shown in blue) indicate scar. Panel B: photograph extracted from the video recorded during the Cox-Maze procedure; Tissue appearing white is the scar. Panel C: Two selected ECGI-reconstructed epicardial electrograms from different sites on the epicardial surface: (a) remote to the scar; (b) within the scar; locations are marked in panel A; LIPV = Left Inferior Pulmonary Vein, LSPV = Left Superior Pulmonary Vein, RIPV = Right Inferior Pulmonary Vein, RSPV = Right Superior Pulmonary Vein, LAA = Left Atrial Appendage, RAA = Right Atrial Appendage.

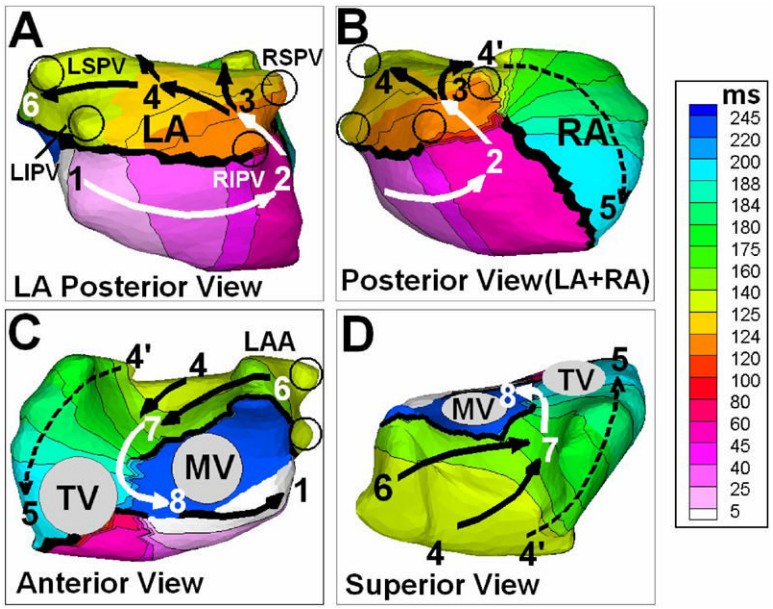

Figure 2.

ECGI reconstructed isochrone map of the flutter cycle. Solid arrows show the reentry circuit. Dashed arrows show a secondary front emanated from the main reentry circuit. The sequence of reentry is 1→2→3→4→(6)→7→8→1. Black circles show locations of the four pulmonary veins. RA = Right Atrium, LA = Left Atrium, MV = Mitral Valve, TV = Tricuspid Valve. LIPV = Left Inferior Pulmonary Vein, LSPV = Left Superior Pulmonary Vein, RIPV = Right Inferior Pulmonary Vein, RSPV = Right Superior Pulmonary Vein, LAA = Left Atrial Appendage.